synchronized saw-tooth sweep voltage wave as the horizontal axis.

It is clear from the resonance condition that the resonant capacitance increases with decreasing the inductance at a given frequency, and we can, therefore, determine the point where the circuit resonates at the moment just before the drop falls. From this value and drop weight, we can easily calculate the specific (differential) capacity per unit area.

Now, the interfacial phase is not equivalent to a simple condenser, but shows several absorption phenomena, which are due to the solution resistance, leakage and the mechanical work of "Counter U-effect", etc. Representing them formally by a series resistance R_{eq}, we can define the "Q-factor" of this circuit by

$$Q = 1/(2\pi f R_{eq} C).$$

From simple calculation this value is shown to be equal to the ratio of the resonant voltage and the applied voltage, which can easily be observed from the amplifier readings.

---

7. Study on Surface Electricity. (XX)

### Capacity Measurement of Dropping Mercury Electrodes by Resonance Method. (2)

Akira Watanabe, Fukuju Tsuji and Shizuo Ueda

(Tachi Laboratory)

The structure of an interfacial double layer is controlled by the applied D. C. polarizing potential and the nature of the ions in solution. One of the most powerful means for studying the ionic behavior in this layer is the determination of the electrical capacity of dropping mercury electrodes. We have made this measurement for several salt solutions by the method described in the preceding article.

The typical shape of the specific capacity per unit area viz. polarizing potential (against electrocapillary maximum potential, i. e. the potential where the electronic charge of mercury surface is zero) is given in Fig. 1. In general, the capacity at anodic polarization is larger than that at cathodic side, which is considered to be due to the fact that anions are generally more easily dehydrated and approach nearer to the mercury surface than cations. The steep rise at extreme cathodic polarization is due to the reversible electrolysis ("pseudo-capacity"). There is a hump near electrocapillary maximum, but in the case of iodides and carbonates we can not find it.

Comparing the shapes of this curve for different electrolytic solutions we can

C_0 μF/cm².

100

80

N. NaCl

C_h

60

40

20

ε_a ε_h

0

0.5   0   -0.5   -1.0   -1.5V.

Polarizing Potential, ε
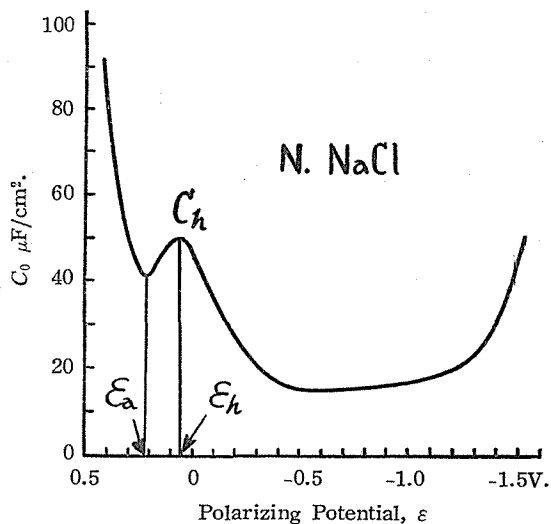
notice some important tendencies. The shape and position of the curve depend chiefly on the nature of the anionic species, cations playing little role for them. The capacity at extreme anodic polarization shows following series,

$$I' > \frac{1}{2} CO_3'' > Br' > Cl' > F' > \frac{1}{2} SO_4'' > ClO_3' > NO'_3.$$

This series is said to be eqal to that of the bond strength between merury and the corresponding anion. (Grahame, Chem. Rev., **41**, 441 (1947)). Several values of the results of experiments are listed in Table 1. From these figures we can see that the

Table 1.

Cations \ Anions		I'	Br'	Cl'	F'	$\frac{1}{2}SO_4''$	NO$_3$'	$\frac{1}{2}CO_3''$	ClO'$_3$
H·	ε_a(v.)			+0.25		+0.37	+0.30		
	ε_h(v.)			+0.08		+0.13	−0.06		
	$C_h(\mu F)$			44.5		35.5	35.0		
K·	ε_a	+0.12	+0.20	+0.21	+0.45	+0.35			+0.22
	ε_h	+0.06	+0.10	+0.08	+0.32	−0.03			−0.03
	C_h	60.5	52.0	32.0	48.0	33.5			30.0
Na·	ε_a	+0.13	+0.23		+0.36	+0.34			
	ε_h	+0.06	+0.05		+0.25	0.00			
	C_h	54.5	50.0		47.0	44.5			
NH$_4$·	ε_a	0.00	+0.23		+0.47	+0.38			
	ε_h	−0.08	+0.09		+0.34	−0.04			
	C_h	58.0	51.5		45.5	35.0			

potential of the peak of humps, ε_h is independent of the nature of cations and has almost equal values for a given anionic species, although some exceptions can be found. ε_a is the potential at which the anodic rise begins, and shows the series,

$$Br' < Cl' < F' < ClO_3' < NO_3' < \frac{1}{2} SO_4''.$$
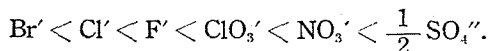
This series is equal to that of the anionic hydration entropies. That is, ε_a is more anodic as the corresponding anion is more difficult to be dehydrated. C_h, the capacity at hump, shows the following series,

$$Br' > Cl' > \frac{1}{2} SO_4'' > NO_3' > F' > ClO_3'$$
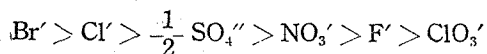
This series is equal to that of the anionic deformability.

These features give important suggestions for the structure of the double layer. We are now developing its analysis, which will be presented in the next article.

---

8. The Transformation of Cu-phthalocyanine Crystal

Electron Microscope and X-ray Diffraction Study

Fiji SUITO, Natsu UYEDA and Hiroshi SHIBANUMA

(Suito Laboratory)

The crystal growth of Cu–phthalocyanine suspended in some aromatic solvents was investigated. The original particles purified by dispersing the conc. H_2SO_4 solution into water are small flakes (Type I). When they are treated in some aromatic solvent such as benzene, toluene, xylene, pyridine, etc., change of shape and size take place and they grow up to some band–shaped flakes (Type II). (See this Bull., **31** (1953)53.) The x–ray diffraction patterns of both type I and II were taken to detect the change in crystal structure by a x–ray camera of Laue type, whose camera length is about 7.5 cm. The wave length of the x–ray used was 1.54 Å of CuK_α line filtered by Ni foil. On the other hand, electron micrographs of those several specimens, whose x–ray patterns were obtained already, were taken by the electron microscope SM–C2. The photo 1 (a) shows that the particles of type I are small flakes, whose size is about 0.05μ in width and 0.4μ in length. The x–ray pattern (b) shows slight diffused lines due to the smallness of the crystal size (type a). The electron micrograph of the specimen treated in toluene at 50°C and elongated to the band-shaped flaky crystals whose size is about 7μ in length and 0.5μ in width, is shown in Fig. 2 (a) and their diffraction pattern in (b), which is different from the one belonging to type a. The number of the detectable diffracted lines was much more increased compared to the former one. This show that the crystal growth to the type II does not take place without accompanied by the crystal structure change.

When the crystals of type I was treated by various kinds of other aromatic sol-